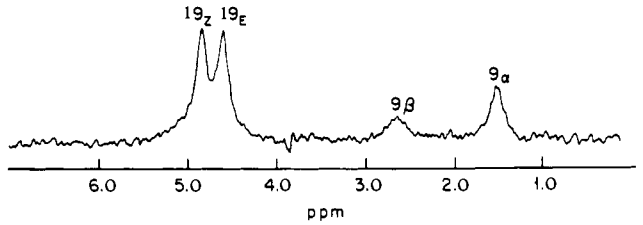

Figure 1. 41.4-MHz ^2H NMR spectrum of [19,19-^2H]vitamin D_3 (**1b**), after 14-h heating at 80 °C.

Table I. Mass Spectrometry of C-19-Deuterated Vitamin D_3 (**1b**). Deuterium Distribution in Fragment a (*m/e* 136–138) at Various Periods of Heating at 80 °C[a]

time, h	ion a deuterium content, %				deuterium label retained in ion a, %[b]
	d_0	d_1	d_2	atoms	
0	9	30	61	1.51[c]	100
2	12	38	50	1.38	91
4	14	45	41	1.27	84
6	16	49	35	1.19	79
8	23	53	24	1.01	66
14	27	52	21	0.94[d]	62

[a] The percentage are corrected for the ^{13}C isotope; estimated error was 7% of the value quoted. [b] Relative to the labeled fragment a, derived from nonequilibrated vitamin D_3. [c] Deuterium content in molecular ion, percent: d_0, 5; d_1, 24; d_2, 71; atoms, 1.66. [d] Deuterium content in molecular ion, percent: d_0, 8; d_1, 24; d_2, 68; atoms, 1.60.

tween C-19 and C-9 was not reached even after 14-h heating.

From the change of distribution of d_0, d_1, and d_2 in the ion a on heating, we have calculated the approximate isotope exchange rate, and found it to be 2.6×10^{-5} s^{-1}, which can be related to the rate of the deuterium transfer from C-19 of **2b** to C-9 of **1b**. Considering that the corresponding rate of protium migration was found to be 1.2×10^{-3} s^{-1},[2] the isotope effect k_H/k_D is ~45.[13]

To establish whether a kinetic preference exists in the previtamin–vitamin reaction, we have measured the ^2H NMR spectra of the deuterium-labeled vitamin **1b**. We have observed two signals whose chemical shifts at 4.7 and 4.9 ppm were identical with those of the protons at C-19 in the ^1H NMR spectrum of the unlabeled vitamin **1a**.[6] After heating for 14 h at 80 °C and separating the vitamin from the reaction mixture, two additional signals appeared at 1.68 and 2.70 ppm, the former identified as the deuteron at C-9α and the latter as the deuteron at C-9β[6b,7] (Figure 1). The integration ratio of the two signals was found to be ~2:1, indicating a preference for deuterium migration to the 9α position.[14] This preference was also observed in the ^2H NMR spectrum after 2-h heating which revealed, in addition to the signals due to ^2H at C-19, also a weak signal at 1.68 ppm of ^2H at C-9α, while the signal due to H at C-9β was undetectable.

It seems reasonable to assume that the transition state for the vitamin D_3–previtamin D_3 isomerization has a preferred conformation, in which the cis-1,3,5-triene system of the two compounds is twisted in a right-handed sense, ring A lying below the plane of the C/D rings.[15]

Acknowledgment. We thank the United States–Israel Binational Science Foundation, Jerusalem, for their financial support.

References and Notes

(1) M. F. Holick, J. Frommer, S. McNeill, N. Richt, J. Henley, and J. T. Potts, Jr., *Biochem. Biophys. Res. Commun.*, **76**, 107 (1977).
(2) J. L. M. A. Schlatmann, J. Pot, and E. Havinga, *Recl. Trav. Chim. Pays-Bas*, **83**, 1173 (1964).
(3) R. B. Woodward and R. Hoffmann, *J. Am. Chem. Soc.*, **87**, 2511 (1965).
(4) M. Akhtar and G. J. Gibbons, *J. Chem. Soc.*, 5964 (1963).
(5) H. H. Inhoffen, K. Irmscher, H. Hirschfeld, U. Stache, and A. Kreutzer, *Chem. Ber.*, **91**, 2309 (1958); B. Lythgoe and I. R. Harrison, *J. Chem. Soc.*, 837, 843 (1958).
(6) (a) G. N. LaMar and D. L. Budd, *J. Am. Chem. Soc.*, **96**, 7317 (1974); (b) R. M. Wing, W. H. Okamura, A. Rego, M. R. Pirio, and A. W. Norman, *J. Am. Chem. Soc.*, **97**, 4980 (1975); (c) E. Berman, Z. Luz, Y. Mazur, and M. Sheves, *J. Org. Chem.*, **42**, 3325 (1977).
(7) Decoupling experiments confirmed the assignment of H at C-9β[6b] and identified H at C-9α.
(8) The shape of the proton signal at C-9β which appears as a well-resolved doublet with $^2J_{9\beta\text{-}9\alpha}$ = 11 Hz (with small splitting due to vicinal coupling) changes after thermal equilibration, showing an additional superimposed narrow doublet ($J < 2$ Hz, ^1H–^2H vicinal coupling). This indicates that the 9α position is partially occupied by deuterium, which migrated from C-19 to both C-9α and C-9β.
(9) J. W. Blunt, H. F. DeLuca, and H. K. Schnoes, *Biochemistry*, **7**, 3317 (1968); W. H. Okamura, M. L. Hamond, H. J. C. Jacobs, and Jan van Thuijl, *Tetrahedron Lett.*, 4807 (1976).
(10) Vitamin D_3 samples were isolated from the reaction mixture after heating, purified, and analyzed by mass spectrometry.
(11) For the method of analysis, cf. L. Tökes, G. Jones, and C. Djerassi, *J. Am. Chem. Soc.*, **90**, 5465 (1968); R. Beugelmans, R. Shapiro, L. Durham, D. Williams, H. Budzikiewicz, and C. Djerassi, *ibid.*, **86**, 2832 (1964).
(12) Similar results were obtained with [19,19-^2H]-3-deoxyvitamin D_3.
(13) A large value of primary isotope effect is expected for hydrogen migration in systems having a nearly linear and symmetrical transition state which includes the previtamin–vitamin system; cf. F. H. Westheimer, *Chem. Rev.*, **61**, 265 (1961); J. Bigeleisen, *Pure Appl. Chem.*, **8**, 217 (1964); H. Kloosterziel and A. P. Ter Borg, *Recl. Trav. Chem. Pays-Bas*, **84**, 1305 (1965); H. Kwart and M. L. Latimore, *J. Am. Chem. Soc.*, **93**, 3770 (1971); and A. W. Pryor and K. G. Kneipp, *ibid.*, **93**, 5584 (1971).
(14) A thermodynamic preference for stereospecific hydrogen migration was observed in analogous thermal reaction of a 1,3,5 triene derived from ursolic acid; cf. R. L. Autrey, D. H. R. Barton, A. K. Ganguly, and W. H. Reusch, *J. Chem. Soc.*, 3313 (1961).
(15) Since both the vitamin and the previtamin are at room temperature in the thermodynamically more stable 6,7 and 5,6 s-trans conformation, respectively, they have to undergo a right-handed rotation about these bonds to adopt such a conformation. This right-handed twist may be energetically preferred to the alternative left-handed twist.

Mordechai Sheves, Elisha Berman, Yehuda Mazur*
Zeev V. I. Zaretskii
Departments of Organic Chemistry and Isotope Research
The Weizmann Institute of Science, Rehovot, Israel
Received September 27, 1978

A Structural Model for the Photosynthetic Reaction Center

Sir:

We describe here the synthesis and characterization of the solution conformation of a molecule which brings into close proximity the principal molecular components believed to participate in the initial photoinduced electron-transfer reaction of photosynthesis. Comparison of the spectroscopic properties of the anion and cation radicals of bacteriochlorophyll and bacteriopheophytin (metal-free bacteriochlorophyll) with optical transients elicited from bacterial photosynthetic reaction centers has led to the widely accepted view that bacteriopheophytin serves as the first electron acceptor following photoexcitation.[1] The photoexcited electron donor has been shown to consist of a pair of bacteriochlorophylls[2] whose detailed structure remains elusive, though the subject of extensive speculation and modeling.[3] The identity of participants in green plant and algal photosynthesis is much less certain owing to the complication of two photosystems and unavailability of simple, low molecular weight reaction centers. In spite of this, an increasing body of evidence is developing which suggests intermediate transient electron acceptors in both photosystem I and II,[4,5] and pheophytin and chlorophyll monomers are very reasonable candidates.[5] The central question which then emerges is the nature of the spatial relationship among these components which facilitates efficient forward electron transfer, and synthetic model compounds can provide the first steps toward an answer.

The covalently linked array of metal-containing and metal-free pyrochlorophyll macrocycles[6] shown in Figure 1

0002-7863/79/1501-1883$01.00/0

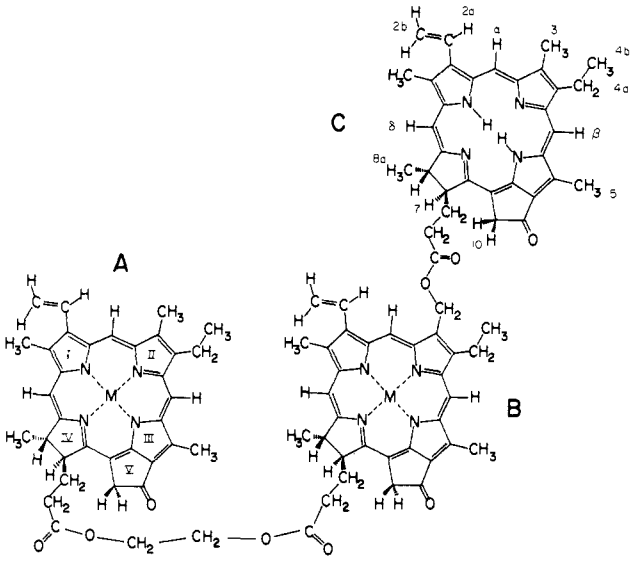

Figure 1. Structure, ring labels, and numbering system for synthetic models; M = Zn or Mg.

Table I. Magnitudes of Largest Chemical-Shift Changes Accompanying Folding of Model Compounds

proton[a]	Δ chemical shift[b]	
	Zn_2 model	Mg_2 model
A-5	+2.53	+2.59
B-5	+1.73	+2.00
A-β	+0.81	+0.58
C-α	+0.76	+0.44
C-4a	+0.64	+0.51
C-β	+0.48	+0.43
C-3	+0.44	+0.35
C-4b	+0.42	+0.25
A-4b	−0.24	−0.38
B-4b	−0.27	−0.31

[a] See Figure 1 for numbering. [b] Data for solutions which are 1.8×10^{-3} M (C_6D_6) with Δ chemical shift defined as the chemical shift in parts per million in the presence of pyridine-d_5 minus that in the presence of methanol-d_4.

has been prepared as follows. Pyropheophorbides *a* and *b* (PPa and PPb) are prepared from spinach by standard procedures.[7] PPb is esterified to the glycol monoester (ethylene glycol-HCl, 70 °C), which is coupled to an equivalent of the activated ester of PPa in methylene chloride using 2-chloro-*N*-methylpyridinium iodide at 40 °C[8] to give the A-B linked dimer: ^{1}H NMR ($CDCl_3$) δ 10.9 (s, 1 H, aldehyde), 4.2 (br s, 4 H, glycol link), and all other expected resonances. The aldehyde function at position 3 in ring B is selectively reduced[9,10] (^{1}H NMR ($CDCl_3$) δ 5.6 (s, 2 H, methylene, loss of aldehyde)) and both rings are metalated with either Zn[11] or Mg.[12,13a] To complete the synthesis, a molecule of the activated ester of PPa is coupled to the alcohol at position 3 in ring B.[13b]

Proof that the correct molecule has been synthesized comes from the NMR spectrum of this molecule in pyridine (Figure 2a, vide infra) which exhibits all expected resonances in correct proportion, notably two NH protons from ring C (δ 0.4 and −1.7) and the glycol and methylene[14] linkages (δ 3.8 and 6.3, respectively). Complete unambiguous assignment of resonances in the 360-MHz NMR spectrum is accomplished by substituting perdeuterated PPa[15] in the synthesis for rings A and/or C, decoupling in the enormously complex region between 3.2 and 4.1 ppm, and the fact that proton assignments within each ring are well established.[16]

Striking solvent-dependent chemical-shift differences are observed for these compounds, as shown in Figure 2, which

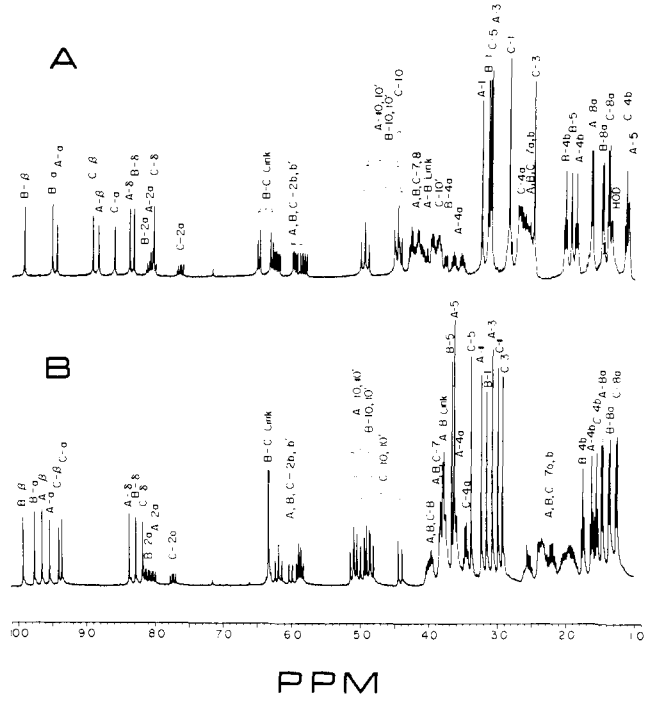

Figure 2. 360-MHz ^{1}H NMR spectra of Zn_2 model, 1.8×10^{-3} M (benzene-d_6) which are (A) 0.6 M in methanol-d_4; (B) 0.3 M in pyridine-d_5. See text for assignments and Table I for magnitudes of largest shift changes. Mg_2 model gives a similar spectrum, but is less well resolved for presentation.

compares the spectrum in the presence of an excess of methanol-d_4[17] and a large excess of pyridine-d_5. The former spectrum is completely assigned by titration to the latter with pyridine,[16] selective deuteration, and decoupling. The assignments are presented in Figure 2 and the magnitudes of the largest chemical-shift changes are tabulated in Table I.

Our structural interpretation of these enormous chemical-shift changes depends on the well-established characteristics of ring-current-induced shifts for this type of macrocycle. Pyridine strongly coordinates the central metal atom, disrupting macrocyclic interactions which depend on metal coordination. By contrast, the large chemical-shift changes in the presence of a hydroxylic ligand indicate specific ligand-mediated interactions. The pattern of chemical-shift changes in rings A and B is similar to what is observed with simpler symmetric dimers: the 5 methyl and 10 protons are shifted upfield while the 4b methyls shift downfield.[3a,c] This combination of shifts is readily shown to be consistent only with an average C_2 symmetrical, folded, solution conformation for this fragment. This structure is stablized by hydrogen bonding to the keto carbonyl group and coordination to the central metal by the hydroxyl-containing ligand. Two striking exceptions to this pattern are the much greater upfield shift for the A-5 methyl relative to B-5 and the A-β upfield shift. To our surprise, several metal-free ring-C protons also exhibit substantial upfield chemical-shift changes, especially the α, β, 4a, 4b, and 10 protons.

All of the chemical-shift data can be combined with the aid of molecular models to provide a unique description of average intermacrocyclic interactions in the presence of methanol as illustrated schematically in Figure 3.[18] Metal-free ring C shows a specific preference to fall over the A ring, causing the upfield shift for the ring A-5 methyl and β protons. The C-10, C-10′ protons are located over the center of ring B, while the C-β proton lies approximately over the center of ring A. The 8a methyl and 8 protons of each macrocycle shift downfield, as predicted from molecular models, as these protons are found in the deshielding region adjacent to another macrocycle. All

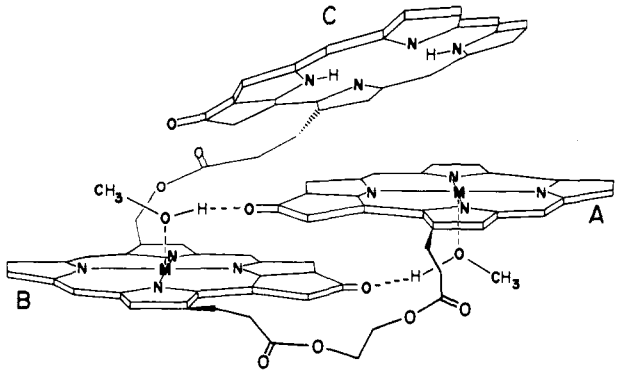

Figure 3. Schematic of average solution structure proposed for Mg_2 and Zn_2 model compounds in the presence of hydroxylic ligands which is consistent with all NMR data.

4a methylene protons are diastereotopic (AB part of an ABX_3 multiplet), with the largest chemical-shift difference in ring A,[19] consistent with their close proximity to two chiral centers in the reduced pyrrole ring of ring C. The distance from a point defined by the intersection of a line drawn between the metals and the C_2 axis of the A–B fragment and the center of ring C is estimated to be ~7–8 Å.[20] Though qualitatively similar the Mg and Zn compounds exhibit a substantial difference in the ease with which the folded form yields to displacement by pyridine. Whereas a 10^2-fold molar excess of pyridine fully disrupts the folded Zn model, a (2×10^3)-fold molar excess is required for the Mg model. We believe that the specificity of the observed interaction between ring C and the A–B fragment is stabilized by the transient substitution of a hydrogen bond between the carbonyl oxygen in ring C and the hydroxyl ligand for the hydrogen bond to the ring-B carbonyl, in concert with π–π interactions.

In contrast to all other porphyrin–protein interactions, where strong axial ligation to the central metal or direct covalent linkages position the macrocycle in combination with nonpolar interactions, there is no evidence for a covalent linkage between chlorophyll or pheophytin and reaction center proteins. Presumably, nonpolar interactions and weak coordination to the central magnesium atom (for the chlorophylls) play crucial roles in determining reaction center chromophore structure.[21] Therefore an analysis of ligand-mediated spontaneous self-assembly among components which are crucial to the primary photochemistry can provide a useful working model for their relationship in vivo. These molecules provide a model of defined structure which is amenable to study, and we are encouraged by the remarkable strength and specificity of the interactions. In a forthcoming paper, we will report a detailed analysis of the photochemistry and photophysics of these molecules[22] with particular emphasis on time-resolved optical absorption, emission, and ESR spectroscopy, which have been widely applied to in vivo systems, and extensions of the synthesis to bacterial chlorophylls and secondary electron acceptors.

Acknowledgment is made to the donors of the Petroleum Research Fund, administered by the American Chemical Society, and the Stanford Institute for Energy Studies for partial support of this work. The 360-MHz NMR spectra were obtained at the Stanford Magnetic Resonance Laboratory supported by National Science Foundation and National Institutes of Health grants GR23633 and RR00711, respectively.

References and Notes

(1) (a) J. Fajer, D. C. Brune, M. S. Davis, A. Forman, and L. D. Spaulding, *Proc. Natl. Acad. Sci. U.S.A.*, **72**, 4956 (1975); (b) P. L. Dutton, R. C. Prince, D. M. Tiede, K. M. Petty, K. J. Kaufmann, T. L. Netzel, and P. M. Rentzepis, *Brookhaven Symp. Biol.*, **28**, 213 (1976); (c) J. Fajer, M. S. Davis, D. C. Brune, A. Forman, and J. P. Thornber, *J. Am. Chem. Soc.*, **100**, 1918 (1978).

(2) (a) J. D. McElroy, G. Feher, and D. C. Mauzerall, *Biochim. Biophys. Acta*, **267**, 363 (1972); (b) J. R. Norris, M. E. Druyan, and J. J. Katz, *J. Am. Chem. Soc.*, **95**, 1680 (1973).

(3) (a) S. G. Boxer and G. L. Closs, *J. Am. Chem. Soc.*, **98**, 5406 (1976); (b) M. R. Wasielewski, U. H. Smith, B. T. Cope, and J. J. Katz, *ibid.*, **99**, 4172 (1977); (c) M. R. Wasielewski, M. H. Studier, and J. J. Katz, *Proc. Natl. Acad. Sci. U.S.A.*, **73**, 4282 (1976); (d) F. K. Fong, *J. Am. Chem. Soc.*, **97**, 6890 (1975).

(4) (a) P. Heathcote, D. L. Williams-Smith, and M. C. W. Evans, *Biochem. J.*, **170**, 373 (1978); (b) G. C. Dismukes, A. McGuire, R. Blankenship, and K. Sauer, *Biophys. J.*, **21**, 239 (1978); (c) S. Demeter and B. Ke, *Biochim. Biophys. Acta*, **462**, 770 (1977).

(5) I. Fugita, M. S. Davis, and J. Fajer, *J. Am. Chem. Soc.*, **100**, 6280 (1978).

(6) Pyrochlorophylls are used to avoid the enormous complexity of the NMR spectra which accompanies unavoidable epimerization at position 10 in ordinary chlorophylls.

(7) H. H. Strain and W. A. Svec in "The Chlorophylls", L. P. Vernon and G. R. Seeley, Eds., Academic Press, New York, 1966, Chapter 2.

(8) T. Mukaiyama, M. Usui, and K. Saigo, *Chem. Lett.*, 49 (1976).

(9) R. F. Borch, M. D. Bernstein, and H. D. Durst, *J. Am. Chem. Soc.*, **93**, 2897 (1971). The $Na{\cdot}BH_3CN$ method is a substantial improvement over $NaBH_4$; cf. A. S. Holt, *Plant Physiol.*, **34**, 310 (1959).

(10) Reduction of the conjugated aldehyde renders the absorption spectrum of ring B indistinguishable from that of ring A. As a consequence, all rings are chlorophyll *a* macrocycles, with minor differences in proton chemical shifts which are very useful for assigning individual protons.

(11) G. R. Seeley in "The Chlorophylls", L. P. Vernon and G. R. Seeley, Eds., Academic Press, New York, 1966, Chapter 3, p 78.

(12) M. R. Wasielewski, *Tetrahedron Lett.*, **No. 16**, 1373 (1977).

(13) (a) Purification: Zn, preparative silica TLC, 250 μ, 2:1 CCl_4–acetone, r_f = 0.28; Mg, preparative Florisil TLC, 1000 μ, 2:1 ethyl acetate–cyclohexane, r_f = 0.40. (b) Purification: same as for precursor; Zn, r_f = 0.52; Mg, r_f = 0.32.

(14) The methylene proton chemical shift in the linkage between the B and C rings is very sensitive both to esterification and the presence of metal in ring B, and comparison with simple models confirms that both conditions are met.

(15) Merck Isotopes Ltd.

(16) G. L. Closs, J. J. Katz, F. C. Pennington, M. R. Thomas, and H. H. Strain, *J. Am. Chem. Soc.*, **85**, 3809 (1963).

(17) In wet solvents, somewhat different chemical shifts are observed. Assignment of the spectrum and structure awaits further experimentation.

(18) The pattern of chemical-shift changes is independent of concentration, which rules out a significant contribution to the shifts from intermolecular aggregation.

(19) 4a methylene proton chemical-shift differences (parts per million): A-4a (0.12) > C-4a (0.09) > B-4a (0.07). Also it is noted that the B–C link methylene protons (position 3, ring B) become measureably diastereotopic (shift difference 0.20 ppm).

(20) To date there has been no direct experimental determination of the distance between the pair of chlorophylls and the primary acceptor in either bacterial or green plant photosynthesis. In bacterial reaction centers, the observed temperature independence of the upper limit for the formation time of the radical ion pair can be related to distance in the framework of the theory of electron tunneling, assuming a thermally relaxed precursor excited singlet state; cf. K. Peters, P. Avouris, and P. M. Rentzepis, *Biophys. J.*, **23**, 207 (1978). Though no distance is specified, the authors cautiously suggest that it is shorter than the distance between bacteriopheophytin and ubiquinone, estimated at 9–13 Å. Also, the apparently negligible electron–electron exchange coupling in the primary radical ion pair can be taken to indicate a substantial separation between donor and acceptor; cf. H.-J. Werner, K. Schulten, and A. Weller, *Biochim. Biophys. Acta*, **502**, 255 (1978).

(21) The existence of a high level of structure among bacterial reaction center chromophores has been elegantly demonstrated optically by A. Vermeglio and R. K. Clayton, *Biochim. Biophys. Acta*, **449**, 500 (1976), and by high resolution photoselection experiments in our laboratory, S. G. Boxer and M. G. Roelofs, submitted for publication.

(22) The absorption spectrum of the folded form of the model is a superposition of the spectra of the metal-free ring and folded dimer components (red absorption maxima at 673 and 692 nm). Fluorescence emission for the folded form of the model occurs exclusively from the folded dimer portion (maximum at 717 nm) irrespective of excitation wavelength, indicating efficient intramolecular energy transfer. The fluorescence quantum yield following excitation at 420 nm is reduced by a factor of two for the folded Mg_2 model relative to an identically absorbing 1:1 mixture of metal-free monomer and folded dimer.

Steven G. Boxer,* Rodney R. Bucks
Department of Chemistry, Stanford University
Stanford, California 94305
Received November 8, 1978

On the Ease of Base-Catalyzed Epimerization of N-Methylated Peptides and Diketopiperazines

Sir:

N-Methylation of peptides promotes base-catalyzed epimerization at the adjacent C_α position,[1] complicating the

0002-7863/79/1501-1885$01.00/0